STRUCTURAL BIOLOGY COMMUNICATIONS

ISSN: 2053-230X
journals.iucr.org/f

Expression, purification, crystallization and preliminary X-ray diffraction analysis of a type II NADH:quinone oxidoreductase from the human pathogen *Staphylococcus aureus*

Ana Lúcia Rosário, Filipa V. Sena, Ana P. Batista, Tânia F. Oliveira, Diogo Athayde, Manuela M. Pereira, José A. Brito and Margarida Archer

Acta Cryst. (2015). F**71**, 477–482

STRUCTURAL BIOLOGY COMMUNICATIONS

ISSN 2053-230X

Expression, purification, crystallization and preliminary X-ray diffraction analysis of a type II NADH:quinone oxidoreductase from the human pathogen *Staphylococcus aureus*

Ana Lúcia Rosário,‡ Filipa V. Sena,‡ Ana P. Batista, Tânia F. Oliveira, Diogo Athayde, Manuela M. Pereira, José A. Brito* and Margarida Archer

Instituto de Tecnologia Química e Biológica – António Xavier, Universidade Nova de Lisboa, Avenida República, 2780-157 Oeiras, Portugal. *Correspondence e-mail: jbrito@itqb.unl.pt

Received 13 February 2015
Accepted 13 March 2015

Edited by M. S. Weiss, Helmholtz-Zentrum Berlin für Materialien und Energie, Germany

‡ Both authors contributed equally to this work.

Keywords: NDH-II; NADH dehydrogenase; respiratory chain; *Staphylococcus aureus*.

Supporting information: this article has supporting information at journals.iucr.org/f

In recent years, type II NADH dehydrogenases (NDH-IIs) have emerged as potential drug targets for a wide range of human disease causative agents. In this work, the NDH-II enzyme from the Gram-positive human pathogen *Staphylococcus aureus* was recombinantly expressed in *Escherichia coli*, purified, crystallized and a crystallographic data set was collected at a wavelength of 0.873 Å. The crystals belonged to the orthorhombic space group $P2_12_12_1$, with unit-cell parameters a = 81.8, b = 86.0, c = 269.9 Å, contained four monomers per asymmetric unit and diffracted to a resolution of 3.32 Å. A molecular-replacement solution was obtained and model building and refinement are currently under way.

1. Introduction

Staphylococcus aureus is an extremely versatile Gram-positive pathogen capable of causing infections that range from minor to life-threatening, such as bacteraemia or endocarditis, with high morbidity and mortality rates (Pereira *et al.*, 2007). In 2010, it was estimated that *S. aureus* caused more deaths than AIDS in the USA. Besides its virulence, *S. aureus* is well known because of its increasing resistance to virtually all classes of antibiotics. Methicillin-resistant *S. aureus* (MRSA) strains are one of the most important causes of antibiotic-resistant nosocomial infections worldwide and have recently also appeared in the community (Pereira *et al.*, 2007).

Three types of NADH:quinone oxidoreductases (NDHs) can be present in respiratory chains: proton-pumping NDHs (or NDH-Is), nonproton-pumping NDHs (also called type II NDHs or NDH-IIs) and sodium-pumping NDHs (or Na^+-Nqrs) (Yagi *et al.*, 2004; Friedrich *et al.*, 1998; Pereira *et al.*, 2004; Steuber, 2001; Steuber *et al.*, 2014). Type II NADH:-quinone oxidoreductases (NDH-IIs) are monotopic membrane proteins containing one flavin adenine dinucleotide (FAD) molecule as the sole redox cofactor (Yagi *et al.*, 2004). These enzymes do not translocate protons and are thus also called alternative, or nonpumping, NADH dehydrogenases. They play a key role in bioenergetics, since many organisms rely solely on them to oxidize NADH and reduce the quinone pool. Moreover, these enzymes have been proposed to functionally substitute complex I-deficient mitochondria, which makes NDH-IIs putative targets for gene therapy (Bai *et al.*, 2001). In recent years, NDH-II enzymes have also emerged as potential drug targets for treatments against *Plasmodium falciparum* (Fisher *et al.*, 2007; Dong *et al.*, 2009; Biagini *et al.*, 2012), the agent that causes malaria, and

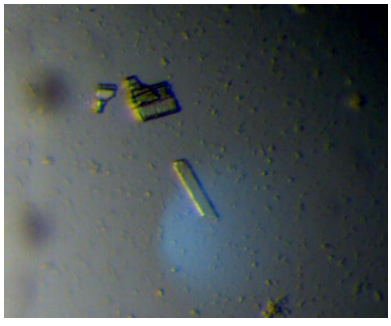

Table 1
Macromolecule-production information.

Source organism	*S. aureus*
DNA source	Genomic
Forward primer	CGTCATATGATGGCTCAAGATC
Reverse primer	CGGCTCGAGCTAGAATTTACCT
Cloning vector	pET-28a(+)
Expression vector	pET-28a(+)
Expression host	*E. coli* Rosetta 2 (DE3)pLysS
Complete amino-acid sequence of the construct produced	HHHHHHMAQDRKKVLVLGAGYAGLQTVTKLQKAI-STEEAEITLINKNEYHYEATWLHEASAGTLNY-EDVLYPVESVLKKDKVNFVQAEVTKIDRDAKK-VETNQGIYDFDILVVALGFVSETFGIEGMKDH-AFQIENVITARELSRHIEDKFANYAASKEKDD-NDLSILVGGAGFTGVEFLGELTDRIPELCSKY-GVDQNKVKITCVEAAPKMLPMFSEELVNHAVS-YLEDRGVEFKIATPIVACNEKGFVVEVDGEKQ-QLNAGTSVWAAGVRGSKLMEESFEGVKRGRIV-TKQDLTINGYDNIFVIGDCSAFIPAGEERPLP-TTAQIAMQQGESVAKNIKRILNGESTEEFEYV-DRGTVCSLGSHDGVGMVFGKPIAGKKAAFMKK-VIDTRAVFKIGGIGLAFKKGKF

Mycobacterium tuberculosis (Yano *et al.*, 2006; Teh *et al.*, 2007), the agent that causes tuberculosis. Interestingly, NDH-II enzymes are absent in mammals and are the only NADH:quinone oxidoreductases that are expressed in some pathogenic microorganisms such as *S. aureus*. Hence, these enzymes arise as promising targets for new antibiotics (Cook *et al.*, 2014; Farha *et al.*, 2013).

Here, we describe the production, crystallization and preliminary crystallographic analysis of *S. aureus* NDH-II. The protein crystallized in space group $P2_12_12_1$ with four molecules in the asymmetric unit. Initial crystallization trials using a Cartesian robot dispensing system yielded crystals in a wide variety of polyethylene glycol (PEG)-containing crystallization conditions. Upscaling these first crystallization hits with hand-made grid screens yielded crystals with poor diffraction quality. Streak-seeding was used to improve the quality of these crystals, rendering new crystals which diffracted to 3.32 Å resolution. A complete crystallographic data set was collected, a molecular-replacement solution was obtained and model building and refinement are currently under way.

2. Materials and methods

2.1. Cloning, overexpression and purification

The gene SAOUHSC_00878 coding for the *S. aureus* NCTC8325 NDH-II was cloned into pET-28a(+) between *Nde*I and *Xho*I restriction sites at the 5′ and 3′ ends, respectively, engineering the addition of a six-residue histidine tag at the N-terminus (Table 1). The gene product corresponds to a 408 amino-acid residue protein with a theoretical molecular mass of ∼45.6 Da. *Escherichia coli* Rosetta 2 (DE3)pLysS cells were transformed with the vector *ndh-S. aureus* and the cells were grown in 2×YT-rich medium supplemented with 100 µg ml^{-1} kanamycin and 34 µg ml^{-1} chloramphenicol at 37°C and 180 rev min^{-1}. Gene expression was induced by the addition of 1 m*M* IPTG (isopropyl β-D-1-thiogalactopyranoside) when the cells reached an OD_{600} of 0.6. The cells were harvested 4 h after induction by centrifugation at 8000 rev min^{-1} for 10 min. The pellets were then resuspended in 100 m*M* K_2HPO_4/KH_2PO_4 pH 7.0, 250 m*M* NaCl containing one cOmplete protease-inhibitor cocktail tablet (Roche) and disrupted in a French press at 41.4 MPa. Cellular debris and undisrupted cells were separated by centrifugation at 10 000 rev min^{-1} for 10 min. The resulting suspension was ultracentrifuged at 42 000 rev min^{-1} for 2 h. The membrane pellet was resuspended with an homogenizer in 100 m*M* K_2HPO_4/KH_2PO_4 pH 7.0, 2 *M* NaCl and incubated overnight at 4°C. No detergents were used during the solubilization and purification of the enzyme (see below). The membrane fraction was again ultracentrifuged at 42 000 rev min^{-1} for 1 h. The NaCl concentration of the supernatant containing NDH-II was decreased to approximately 50 m*M* NaCl at 4°C by successive additions of 100 m*M* K_2HPO_4/KH_2PO_4 pH 7.0 and concentration in an Amicon system (30 000 MWCO). The sample was injected in an ion-exchange Q-Sepharose High Performance column (GE Healthcare) and eluted with a gradient from 0 to 1 *M* NaCl in 100 m*M* K_2HPO_4/KH_2PO_4 pH 7.0. The fraction containing NDH-II was then applied onto a gel-filtration Superdex 200 XK 26/60 column (GE Healthcare) and eluted with 100 m*M* K_2HPO_4/KH_2PO_4 pH 7.0, 250 m*M* NaCl containing one cOmplete protease-inhibitor cocktail tablet (Roche). The pure protein was stored at −80°C.

Table 2
Crystallization conditions and experimental setup.

Method	Vapour-diffusion (hanging-drop)
Plate type	24-well Linbro Plate
Temperature (°C)	20
Protein concentration (mg ml^{-1})	7
Buffer composition of protein solution	35 m*M* K_2HPO_4/KH_2PO_4 pH 7.0, 175 m*M* NaCl
Composition of drop solution	20%(*w*/*v*) PEG 3350, 0.2 *M* ammonium nitrate
Composition of reservoir solution	26%(*w*/*v*) PEG 3350
Volume and ratio of drop	2 µl (1 µl protein solution + 1 µl precipitant)
Volume of reservoir (ml)	1

2.2. Crystallization

Initial crystallization trials were performed at 20°C with a 10 mg ml^{-1} NDH-II solution in 100 m*M* K_2HPO_4/KH_2PO_4 pH 7.0, 250 m*M* NaCl by the sitting-drop vapour-diffusion technique using a Cartesian robot dispensing system (Mini-Bee, Genomic Solutions). Two commercially available crystallization screens (PACT Premier and JCSG+ from Molecular Dimensions) were used; 200 nl drops with a 1:1 ratio of protein and precipitant solutions were set up in 96-well flat-bottom plates (Greiner Bio-One) and equilibrated against a reservoir consisting of 40 µl precipitant solution. Crystalline material appeared in several conditions, most of which contained PEG (1500–10 000) as precipitant. A grid screen was performed around a condition comprising 20%(*w*/*v*) PEG 3350, 0.2 *M* sodium acetate using NDH-II at a concentration of 7 mg ml^{-1} in 35 m*M* K_2HPO_4/KH_2PO_4 buffer pH 7.0, 175 m*M* NaCl. The

Table 3
Data collection and processing.

Values in parentheses are for the outer shell.

Diffraction source	ID23-2, ESRF
Wavelength (Å)	0.873
Temperature (°C)	−173
Detector	Pilatus 2M
Crystal-to-detector distance (mm)	384.5
Rotation range per image (°)	0.15
Total rotation range (°)	101.1
Exposure time per image (s)	0.10
Space group	$P2_12_12_1$
a, b, c (Å)	81.8, 86.0, 269.9
α, β, γ (°)	90, 90, 90
Resolution range (Å)	60.5–3.32 (3.33–3.32)
Total No. of reflections	104532 (617)
No. of unique reflections	28851 (264)
Completeness (%)	99.5 (90.4)
Multiplicity	3.6 (2.3)
$\langle I/\sigma(I)\rangle$	8.3 (2.00)
R_{merge}	0.15 (0.49)
R_{meas}	0.18 (0.61)
$R_{p.i.m.}$	0.09 (0.36)
$CC_{1/2}$	0.98 (0.72)
Overall B factor from Wilson plot (Å^2)	60.46

protein solution was mixed in a 1:1 ratio with 18–26%(*w*/*v*) PEG 3350, 0.2 *M* sodium acetate pH 6.5–7.5 solution and equilibrated against 1 ml crystallization solution in the reservoir of a 24-well Linbro plate (Hampton Research). Crystals appeared in 3–4 d by the hanging-drop vapour-diffusion method but showed poor X-ray diffraction quality (maximum resolution of ∼8 Å). These crystals were then used to streak-seed a drop consisting of the protein solution at the same concentration mixed in a 1:1 ratio with 20%(*w*/*v*) PEG 3350, 0.2 *M* ammonium nitrate (solution C3 from the JCSG+ screen) and previously equilibrated for 12 d against 1 ml 26%(*w*/*v*) PEG 3350 by vapour diffusion (Table 2).

2.3. Data collection and processing

Cryoprotection was achieved by transferring the crystals to a 3 µl drop of solution No. 7 from the CryoProtX screen (Molecular Dimensions), consisting of 12.5%(*w*/*v*) diethylene glycol, 12.5%(*w*/*v*) ethylene glycol, 25%(*w*/*v*) 1,2-propanediol, 12.5%(*w*/*v*) dimethyl sulfoxide, 12.5%(*w*/*v*) glycerol. The crystals were flash-cooled by quick plunging into liquid nitrogen. X-ray data were collected from cooled crystals at −173°C on beamlines ID23-1, ID23-2 and ID-29 at the European Synchrotron Radiation Facility (ESRF), Grenoble, France and the PROXIMA1 beamline at the SOLEIL synchrotron, Paris, France. The X-ray data presented here and used for structure determination were collected at a wavelength of 0.873 Å on beamline ID23-2 at the ESRF. X-ray diffraction data were indexed and integrated with *XDS* (Kabsch, 2010); space-group assignment was performed with *POINTLESS* (Evans, 2011) and scaling was performed with *SCALA*/*AIMLESS* (Evans, 2006) within the *autoPROC* data-processing pipeline (Vonrhein *et al.*, 2011). An R_{free}-flagged reflection set was created at this stage corresponding to 5% of the measured reflections for this data set. A summary of the diffraction protocol and data-collection statistics is given in Table 3.

3. Results and discussion

The membrane protein NDH-II from *S. aureus* was heterologously expressed in *E. coli* and purified to homogeneity by two chromatographic steps: anion exchange followed by size exclusion. No detergents were used during the solubilization and purification of NDH-II. The protocols were optimized in order to obtain an NDH-II preparation with full FAD content, *i.e.* NDH-II:FAD in a 1:1 ratio. Initially, several detergents, including *n*-dodecyl-*β*-D-maltoside (DDM), *n*-octyl-*β*-D-glucoside (OG) and Triton X-100, were tested. However, the obtained preparations were unstable, leading to loss of the prosthetic group. Since NDH-II is a monotopic membrane protein (and hence has no transmembrane regions), washing the membranes with 2 *M* NaCl was sufficient to solubilize this membrane-attached protein. This step was revealed to be crucial for two reasons: firstly, it had the advantage of immediately separating all the soluble and integral membrane proteins and, secondly, the obtained preparation was stable and fully loaded with FAD cofactor (data not shown). Notably, this allowed the functional characterization of an NDH-II for the first time without possible interference caused by the presence of detergent. Although the protein was produced with a His_6 tag at the N-terminus, no affinity chromatography step, namely Ni–NTA, was used for the reasons highlighted above, *i.e.* obtaining a preparation with an NDH-II:FAD ratio of 1:1. We have observed that this type of chromatography quite often leads to loss of the prosthetic group as previously reported (Radjendirane *et al.*, 1991), and the reversible dissociation of flavoproteins into the constituents, the apoprotein and the flavin prosthetic group, has received much

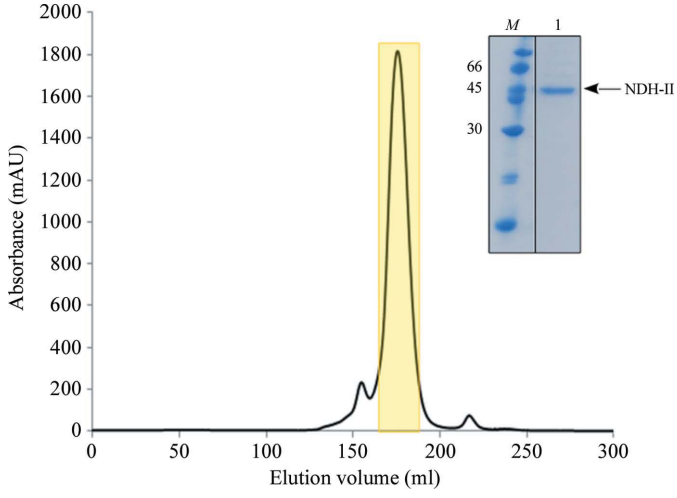

Figure 1
Size-exclusion chromatography and SDS–PAGE analysis (inset) of purified *S. aureus* NDH-II. Lane *M* contains molecular-weight markers and lane 1 contains the peak depicted in yellow in the chromatogram. The dimeric fraction of NDH-II from the size-exclusion column (∼90 kDa) was used for crystallization trials.

attention in the past (Husain & Massey, 1978; Müller & van Berkel, 1991; Lederer *et al.*, 1999). The major elution volume peak in the gel-filtration column corresponds to a dimer in solution with an apparent molecular weight of ∼90 kDa (Fig. 1). The protein identified by mass spectrometry was pure as judged by SDS–PAGE analysis (Fig. 1, inset).

NDH-II crystallized in several conditions, most of which involved polyethylene glycol of different molecular weight as the precipitant, over the course of one week. However, most crystals appeared as small clusters of needles (Fig. 2*a*). Optimization trials involved performing a grid screen around a hand-made condition comprising 20%(*w*/*v*) PEG 3350, 0.2 *M* sodium acetate. The pH was varied from 6.5 to 7.5 and the drops were equilibrated against reservoir solutions consisting of PEG 3350 ranging from 18 to 26%(*w*/*v*). The protein concentration was lowered to 7 mg ml^{-1} in 35 m*M* K_2HPO_4/KH_2PO_4 pH 7.0, 175 m*M* NaCl (in our experience, upscaling directly from robot-made nanodrops yields precipitated drops on most occasions). The crystallization results were not very reproducible and the crystals often appeared as sea-urchin-like agglomerates (Fig. 2*b*) or long, thin needles (Fig. 2*c*). These crystals only diffracted to ∼8 Å resolution using a synchrotron source. We then tried to reproduce the crystallization conditions using 20%(*w*/*v*) PEG 3350, 0.2 *M* ammonium chloride (solution A9 from the JCSG+ screen), 20%(*w*/*v*) PEG 3350, 0.2 *M* ammonium nitrate (solution C3 from the JCSG+ screen), 20%(*w*/*v*) PEG 3350, 0.2 *M* sodium malonate acid pH 7.0 (solution G6 from the JCSG+ screen) and 20%(*w*/*v*) PEG 3350, 0.15 *M* DL-malic acid pH 7.0 (solution G8 from the JCSG+ screen) from the original screen but no crystals appeared. It was decided then to streak-seed these drops with the poor-looking crystals from the hand-made optimization trials. Small rhomboid crystals appeared within 24 h (Fig. 2*d*). These crystals were cryoprotected by transferring them into a solution consisting of 12.5%(*w*/*v*) diethylene glycol, 12.5%(*w*/*v*) ethylene glycol, 25%(*w*/*v*) 1,2-propanediol, 12.5%(*w*/*v*) dimethyl sulfoxide, 12.5%(*w*/*v*) glycerol (solution No. 7 from the CryoProtX screen; Molecular Dimensions) and a complete crystallographic data set was collected on beamline ID23-2 at the ESRF, Grenoble, France (Fig. 3).

The crystals belonged to the orthorhombic space group $P2_12_12_1$, with unit-cell parameters a = 81.8, b = 86.0, c = 269.9 Å, $\alpha = \beta = \gamma = 90^\circ$. Although the merging statistics seem a little high (overall R_{meas} and R_{merge} of 0.18 and 0.15,

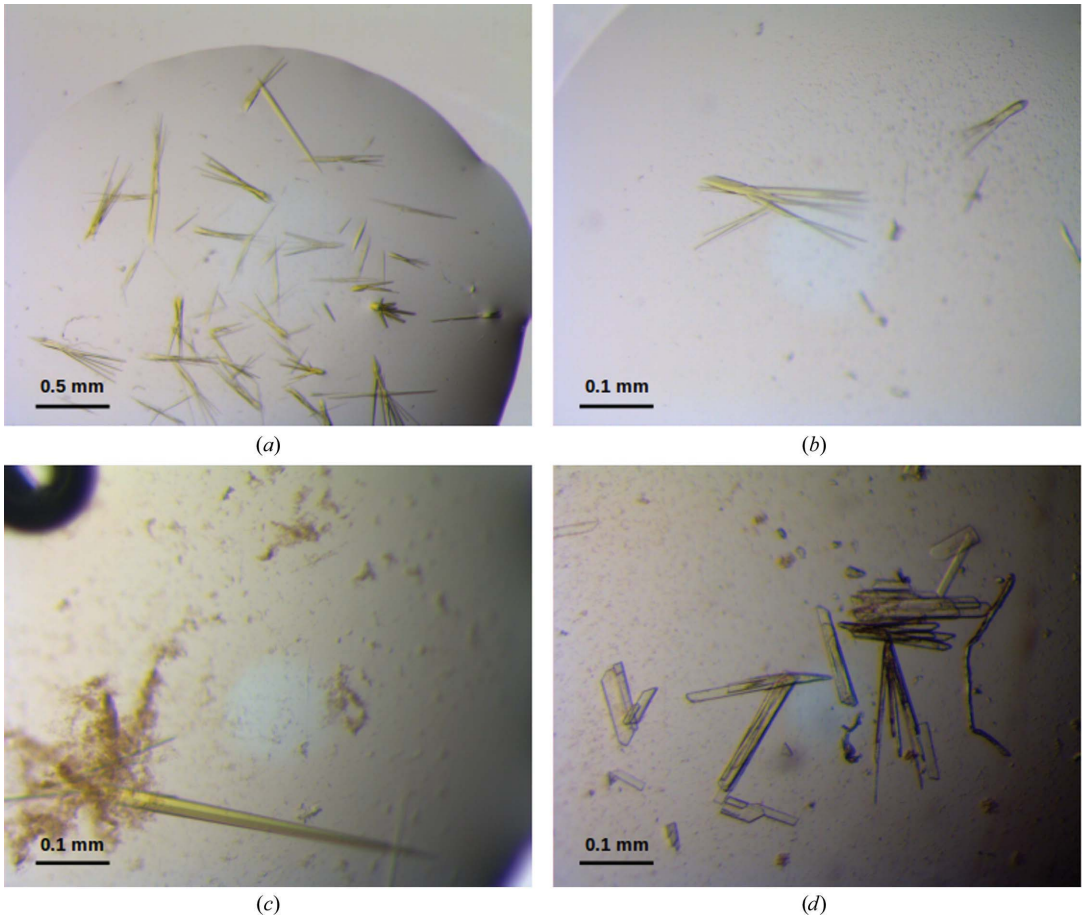

Figure 2
NDH-II crystals grown (*a*), (*b*) during initial crystallization trials using the robot, (*c*) on scaling-up using the hand-made crystallization solution [20%(*w*/*v*) PEG 3350, 0.2 *M* sodium acetate] and (*d*) on scaling-up using solution C3 [20%(*w*/*v*) PEG 3350, 0.2 *M* ammonium nitrate] from the JCSG+ crystallization screen (Molecular Dimensions) and streak-seeding from the crystals in (*c*). The crystals in (*d*) diffracted to 3.32 Å resolution using a synchrotron-radiation source. The crystals are yellow owing to the presence of the FAD prosthetic group.

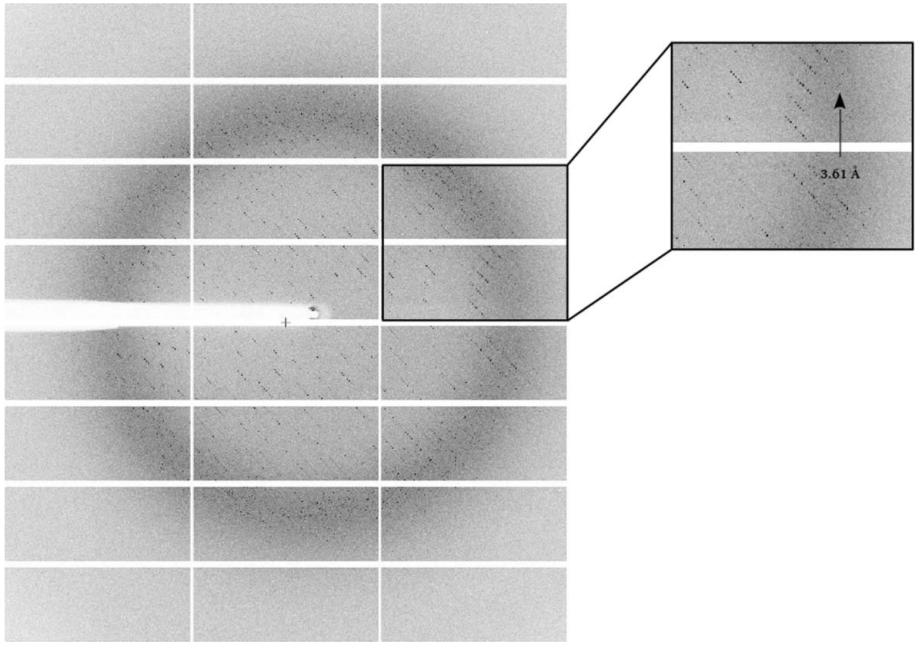

Figure 3
X-ray diffraction image. An X-ray diffraction pattern collected from a single crystal of NDH-II on the ID23-2 beamline at the ESRF. The image was prepared by merging ten consecutive diffraction images (corresponding to 1.5° rotation) with the *MERGE2CBF* program from the *XDS* package. The arrow points to the last visible reflections, although the maximum resolution observed was 3.32 Å (Pilatus 2M detector).

respectively), careful attention was paid to point-group and space-group determination. After processing the data in a triclinic space group, *POINTLESS* (Evans, 2011) was used to assess consistency between symmetry-equivalent reflections and systematically absent reflections. With a probability of 98.5% of a *Pmmm* Laue group and twofold absences verified in the three cell axes, space group $P2_12_12_1$ was clearly identified. Moreover, processing the data in all monoclinic and orthorhombic alternative space groups did not yield better merging statistics. We attribute the high values of $R_{\rm meas}$ and $R_{\rm merge}$ to the quality of the internal organization of the crystal.

Solvent-content analysis (Matthews, 1968) was compatible with the following situations: (i) four molecules in the asymmetric unit, with $V_{\rm M}$ = 2.70 Å^3 Da^{-1} and 54% solvent and (ii) five molecules in the asymmetric unit, with $V_{\rm M}$ = 2.16 Å^3 Da^{-1} and 43% solvent. Before trying any phasing protocols, simply taking into account that NDH-II should be a dimer, the first situation appeared to be the correct one. Phasing was achieved by molecular replacement using *Phaser* (McCoy *et al.*, 2007) within the *PHENIX* suite of programs (Adams *et al.*, 2010). The atomic coordinates of *Caldalkalibacillus thermarum* NDH-II (PDB entry 4nwz; Heikal *et al.*, 2014), without any solvent or prosthetic group molecules, were used as search model (46.0% sequence identity and 66.7% sequence similarity for 185 and 268 aligned amino-acid residues, respectively). The statistics from *Phaser* (McCoy *et al.*, 2007) showed a translation-function *Z*-score of 31.6 and a top LLG score of 1419.1 with four molecules in the asymmetric unit. Searching for a putative fifth molecule yielded no solutions so the molecular-replacement step allowed us to confirm the presence of a tetramer (a dimer of dimers) in the asymmetric unit. Model building and refinement are currently under way, with promising preliminary results (Supplementary Fig. S1).

Acknowledgements

We acknowledge João Carita for cell growth and Pedro Matias for help during data collection. We also acknowledge Susana Lobo and Pedro Matias for critical reading of the manuscript. These experiments were performed on the ID23-2 beamline at the European Synchrotron Radiation Facility (ESRF), Grenoble, France and the PROXIMA1 beamline at the SOLEIL synchrotron, Paris, France. We are grateful to the beamline staff for providing assistance and technical support during diffraction data experiments. JAB and APB are recipients of grants SFRH/BPD/79224/2011 and SFRH/BPD/80741/2011 from Fundação para a Ciência e a Tecnologia, respectively. This project was funded by Fundação para a Ciência e a Tecnologia through grants PTDC/BIA-PRO/118535/2010 to MA, PTDC/BBB-BQB/2294/2012 to MMP and #PEst-OE/EQB/LA0004/2011. MA acknowledges funding from Bio-Struct-X (proposal 1493).

References

Adams, P. D. *et al.* (2010). *Acta Cryst.* D**66**, 213–221.
Bai, Y., Hájek, P., Chomyn, A., Chan, E., Seo, B. B., Matsuno-Yagi, A., Yagi, T. & Attardi, G. (2001). *J. Biol. Chem.* **276**, 38808–38813.
Biagini, G. A. *et al.* (2012). *Proc. Natl Acad. Sci. USA*, **109**, 8298–8303.
Cook, G. M., Greening, C., Hards, K. & Berney, M. (2014). *Adv. Microb. Physiol.* **65**, 1–62.
Dong, C. K., Patel, V., Yang, J. C., Dvorin, J. D., Duraisingh, M. T., Clardy, J. & Wirth, D. F. (2009). *Bioorg. Med. Chem. Lett.* **19**, 972–975.

Evans, P. (2006). *Acta Cryst.* D**62**, 72–82.
Evans, P. R. (2011). *Acta Cryst.* D**67**, 282–292.
Farha, M. A., Verschoor, C. P., Bowdish, D. & Brown, E. D. (2013). *Chem. Biol.* **20**, 1168–1178.
Fisher, N., Bray, P. G., Ward, S. A. & Biagini, G. A. (2007). *Trends Parasitol.* **23**, 305–310.
Friedrich, T., Abelmann, A., Brors, B., Guénebaut, V., Kintscher, L., Leonard, K., Rasmussen, T., Scheide, D., Schlitt, A., Schulte, U. & Weiss, H. (1998). *Biochim. Biophys. Acta*, **1365**, 215–219.
Heikal, A., Nakatani, Y., Dunn, E., Weimar, M. R., Day, C. L., Baker, E. N., Lott, J. S., Sazanov, L. A. & Cook, G. M. (2014). *Mol. Microbiol.* **91**, 950–964.
Husain, M. & Massey, V. (1978). *Methods Enzymol.* **53**, 429–437.
Kabsch, W. (2010). *Acta Cryst.* D**66**, 125–132.
Lederer, F., Rüterjans, H. & Fleischmann, G. (1999). *Methods Mol. Biol.* **131**, 149–155.
Matthews, B. W. (1968). *J. Mol. Biol.* **33**, 491–497.
McCoy, A. J., Grosse-Kunstleve, R. W., Adams, P. D., Winn, M. D., Storoni, L. C. & Read, R. J. (2007). *J. Appl. Cryst.* **40**, 658–674.
Müller, F. & van Berkel, W. J. H. (1991). *Chemistry and Biochemistry of Flavoenzymes*, edited by F. Müller, pp. 261–274. Boca Raton: CRC Press.
Pereira, M. M., Bandeiras, T. M., Fernandes, A. S., Lemos, R. S., Melo, A. M. P. & Teixeira, M. (2004). *J. Bioenerg. Biomembr.* **36**, 93–105.
Pereira, P. M., Filipe, S. R., Tomasz, A. & Pinho, M. G. (2007). *Antimicrob. Agents Chemother.* **51**, 3627–3633.
Radjendirane, V., Bhat, M. A. & Vaidyanathan, C. S. (1991). *Arch. Biochem. Biophys.* **288**, 169–176.
Steuber, J. (2001). *Biochim. Biophys. Acta*, **1505**, 45–56.
Steuber, J., Vohl, G., Casutt, M. S., Vorburger, T., Diederichs, K. & Fritz, G. (2014). *Nature (London)*, **516**, 62–67.
Teh, J.-S., Yano, T. & Rubin, H. (2007). *Infect. Disord. Drug Targets*, **7**, 169–181.
Vonrhein, C., Flensburg, C., Keller, P., Sharff, A., Smart, O., Paciorek, W., Womack, T. & Bricogne, G. (2011). *Acta Cryst.* D**67**, 293–302.
Yagi, T., Di Bernardo, S., Nakamuro-Ogiso, E., Kao, M. C., Seo, B. B. & Matsuno-Yagi, A. (2004). *Respiration in Archaea and Bacteria*, edited by D. Zannoni, pp. 15–40. Dordrecht: Springer.
Yano, T., Li, L.-S., Weinstein, E., Teh, J.-S. & Rubin, H. (2006). *J. Biol. Chem.* **281**, 11456–11463.